JOURNAL OF Materials CHEMISTRY

Synthesis, crystal structure and magnetic properties of new molybdenum(v) phosphates containing Mn^{2+} or Co^{2+} with three-dimensional structures directed by the nature of the transition metal

Charlotte du Peloux,[a] Pierre Mialane,[a] Anne Dolbecq,[a] Jérôme Marrot,[a] Eric Rivière[b] and Francis Sécheresse*[a]

[a]*Institut Lavoisier, IREM, UMR 8637, Université de Versailles Saint-Quentin, 45 Avenue des Etats-Unis, 78035 Versailles, France. E-mail: secheres@chimie.uvsq.fr*
[b]*Laboratoire de Chimie Inorganique, URA CNRS 420, Institut de Chimie Moléculaire d'Orsay, Université Paris-Sud, 91405 Orsay, France*

Received 8th May 2001, Accepted 8th August 2001
First published as an Advance Article on the web 20th September 2001

A new manganese molybdenum(v) hydroxyphosphate, $Na_{15}Mn_{10}[(HPO_4)(PO_4)_3Mo_6O_{12}(OH)_3]_4(PO_4)\cdot 48H_2O$ (**1**), based on the $\{Mn^{II}[P_4Mo_6O_{28}(OH)_3]_2\}^{16-}$ building block has been synthesized hydrothermally and its structure solved by single-crystal X-ray diffraction. Its structure consists of linear manganese phosphate tetramers with edge sharing manganese octahedra. Four tetramers are connected *via* a phosphato group lying on a $\bar{4}$ axis, leading to infinite chains of manganese to which $\{Mn^{II}[P_4Mo_6O_{28}(OH)_3]_2\}^{16-}$ anions are anchored. The variable temperature magnetic susceptibility data for **1** were fitted with a model taking into account only magnetic interactions arising betweeen manganese sharing oxygen atoms. Thus, the spin Hamiltonian $\hat{H}_S = -J_1(\hat{S}_1\hat{S}_2 + \hat{S}_3\hat{S}_4) - J_2\hat{S}_2\hat{S}_3$ was used, and the best fit was found for $g = 2.018$, $J_1 = -1.09\ cm^{-1}$ and $J_2 = -3.65\ cm^{-1}$, showing the antiferromagnetic character of the exchange interactions in **1**. Attempts to obtain the analogous cobalto compound led to the cobalt molybdenum(v) phosphate $Na_{12}Co_3[(PO_4)_4Mo_6O_{12}(OH)_3]_2\cdot 44H_2O$ (**2**). **1** and **2** present two radically different three-dimensional structures. In **2**, the $\{Co[P_4Mo_6O_{28}(OH)_3]_2\}^{16-}$ units are connected *via* monomeric Co^{2+} in an octahedral environment to give a three-dimensional framework, with long Co^{2+}–Co^{2+} distances. The sodium counter-ions are located in tunnels running along the [001] and [010] axes. This clearly shows that the three-dimensional structure is determined by the nature of the transition metal.

Introduction

Reduced molybdenum phosphates, based on the association of $\{Mo^{V}_2O_4\}$ fragments and PO_4 tetrahedra, constitute a large class of compounds, with structures ranging from one-dimensional polymers to three-dimensional microporous materials which are particularly attractive for applications in catalysis, ion exchange and molecular sieves.[1] Among the molybdenum phosphates characterized, the recurrent anionic building unit $[P_4Mo_6O_{28}(OH)_3]^{9-}$, denoted P_4Mo_6, is encountered, with degrees of protonation varying from one structure to the next.[2] We have recently described the synthesis of the analogous oxothioanion $[P_4Mo_6S_6O_{22}(OH)_3]^{9-}$, easily prepared in solution under mild conditions starting from the previously reduced $[Mo^{V}_2S_2O_2]^{2+}$ thiocation.[3] However, hydrothermal synthesis is usually the method of choice for the preparation of reduced molybdenum phosphate oxoanions, with organic amines often used as templates. We are currently investigating the Mo/P/M (M = transition metal cation) system by hydrothermal synthesis, with the aim to obtain multidimensional molybdenum phosphate frameworks showing magnetic properties. We have thus recently prepared a new family of cobalto-phosphates, containing the new $[H_{14}(Mo_{16}O_{32})Co_{16}(PO_4)_{24}(H_2O)_{20}]^{10-}$ building group, and relatively strong antiferromagnetic coupling has been found between the Co^{2+} ions.[4] In all the reported compounds based on the P_4Mo_6 unit and containing additional transition metals, the active magnetic centers are well isolated from one another. We have thus decided to work in high M^{2+}/P_4Mo_6 (M = Mn, Co) ratio conditions, in order to obtain compounds possessing magnetic properties and containing the highly stable P_4Mo_6 building group. Here we report the syntheses and structural characterizations of two new molybdenum phosphates. In $Na_{15}Mn_{10}[(HPO_4)(PO_4)_3Mo_6O_{12}(OH)_3]_4(PO_4)\cdot 48H_2O$ (**1**), a phosphate group connects four tetramers of Mn^{2+} ions, leading to infinite chains of manganese to which the P_4Mo_6 units are anchored *via* phosphate groups. The magnetic study of compound **1** is reported. Attempts to obtain the analogous cobalto compound led to $Na_{12}Co_3[(PO_4)_4Mo_6O_{12}(OH)_3]_2\cdot 44H_2O$ (**2**), which exhibits a different three-dimensional structure. In **2**, the P_4Mo_6 cores are linked by monomeric Co^{2+} ions, with long Co^{2+}–Co^{2+} distances.

Experimental

A mixture of $Na_2MoO_4\cdot 2H_2O$ (0.47 g, 1.94 mmol), Mo (0.03 g, 0.30 mmol), H_3PO_4 8 M (0.53 mL, 4.22 mmol), $MnCl_2\cdot 4H_2O$ (0.17 g, 0.86 mmol), iminodiacetic acid (0.20 g, 1.50 mmol) and water (4 mL) (pH = 5.5 adjusted with NaOH 1 M) was sealed in a 23 cm^3 Teflon-lined reactor which was kept at 180 °C for 70 h. Dark red parallepipedic crystals were obtained as a single phase, in good yield (40%, based on Mo). IR (KBr pellets, ν/cm^{-1}): 1137 (m), 1113 (m), 1055 (s), 1014 (s), 971 (m), 958 (s), 922 (m), 727 (m), 699 (m), 615 (w), 548 (w), 494 (m), 386 (m). $H_{108}Mn_{10}Mo_{24}Na_{15}O_{174}P_{17}$: calcd. Mn 8.25, Mo 34.60, Na 5.18, P 7.92; found Mn 7.79, Mo 32.53, Na 5.29, P 7.92%.

Compound **2** was synthesized by a similar procedure starting from a mixture of $Na_2MoO_4\cdot 2H_2O$ (0.47 g, 1.94 mmol), Mo (0.03 g, 0.30 mmol), H_3PO_4 8 M (0.53 mL, 4.22 mmol), $CoCl_2\cdot 6H_2O$ (0.21 g, 0.88 mmol), iminodiacetic acid (0.20 g, 1.50 mmol) and water (4 mL) (pH = 5.5, adjusted with NaOH 1 M). Red parallelepipedic crystals of **2** were isolated from a

 DOI: 10.1039/b104030h

Table 1 Crystallographic data for **1** and **2**

	1	**2**
Formula	$H_{90}Mn_{10}Mo_{24}Na_{10}O_{165}P_{17}$	$H_{86}Co_3Mo_{12}Na_{12}O_{102}P_8$
M/g mol^{-1}	6338.3	3570.4
Crystal system	tetragonal	monoclinic
Space group	$I4_1/acd$	$C2/m$
a/Å	27.1925(3)	28.1613(2)
b/Å	$b=a$	14.2131(1)
c/Å	41.0974(5)	12.9980(1)
β/°	90	114.79(1)
V/Å^3	30388.7(6)	4723.2(1)
Z	8	2
μ/mm^{-1}	3.046	2.374
Reflections collected	100570	16810
Unique data (R_{int})	10646 (0.0640)	6451 (0.0242)
Parameters	602	342
R_1, wR_2 [$I>2\sigma(I)$]	0.0393, 0.1049	0.0322, 0.0947

Table 2 Selected bond lengths (Å) in **1** and **2**

1			
Mo1A–O1A	1.675(4)	Mo3B–O10	1.948(3)
Mo1A–O8A	1.941(3)	Mo3B–O12	1.971(3)
Mo1A–O11A	1.978(3)	Mo3B–O6B	2.051(3)
Mo1A–O4A	2.039(4)	Mo3B–O9B	2.126(3)
Mo1A–O7	2.091(3)	Mo3B–O14B	2.232(3)
Mo1A–O13	2.326(3)	P1–O15	1.499(4)
Mo1A–Mo2A	2.5986(6)	P1–O14A	1.557(3)
Mo1B–O1B	1.688(4)	P1–O13	1.558(3)
Mo1B–O8B	1.941(3)	P1–O14B	1.559(3)
Mo1B–O11B	1.974(3)	P2–O16	1.503(4)
Mo1B–O4B	2.035(3)	P2–O17	1.521(4)
Mo1B–O7	2.114(3)	P2–O4B	1.552(4)
Mo1B–O13	2.271(3)	P2–O4A	1.558(4)
Mo1B–Mo2B	2.6028(6)	P3A–O18A	1.510(4)
Mo2A–O2A	1.682(4)	P3A–O19A	1.520(4)
Mo2A–O8A	1.939(3)	P3A–O6A	1.551(4)
Mo2A–O11A	1.976(3)	P3A–O5A	1.556(4)
Mo2A–O5A	2.027(4)	P3B–O19B	1.502(4)
Mo2A–O9A	2.107(3)	P3B–O18B	1.527(4)
Mo2A–O14A	2.272(3)	P3B–O6B	1.534(4)
Mo2B–O2B	1.685(4)	P3B–O5B	1.540(4)
Mo2B–O8B	1.950(3)	P4–O20	1.543(6)
Mo2B–O11B	1.971(3)	Mn1–O11A	2.168(3)
Mo2B–O5B	2.054(4)	Mn1–O11B	2.185(3)
Mo2B–O9B	2.105(3)	Mn1–O12	2.210(3)
Mo2B–O14B	2.279(3)	Mn2–O18B	2.153(5)
Mo3A–O3A	1.684(4)	Mn2–O15	2.162(4)
Mo3A–O10	1.948(3)	Mn2–O16	2.194(4)
Mo3A–O12	1.976(3)	Mn2–O2W	2.231(4)
Mo3A–O6A	2.056(4)	Mn3–O17	2.063(5)
Mo3A–O9A	2.111(4)	Mn3–O19B	2.105(5)
Mo3A–O14A	2.269(3)	Mn3–O18B	2.329(5)
Mo3A–Mo3B	2.5972(6)	Mn3–O19B	2.433(6)
Mo3B–O3B	1.686(4)	Mn3–O9WA	2.468(13)
2			
Mo1–O1	1.683(3)	Mo3–O14	2.290(3)
Mo1–O8	1.941(3)	Mo3–Mo3	2.5874(6)
Mo1–O11	1.977(3)	Mo1C–O1C	1.684(5)
Mo1–O4	2.028(3)	P1–O15	1.515(4)
Mo1–O7	2.093(2)	P1–O14	1.549(3)
Mo1–O13	2.267(2)	P1–O13	1.555(4)
Mo1–Mo2	2.6003(4)	P2–O16	1.512(4)
Mo2–O2	1.679(3)	P2–O17	1.519(4)
Mo2–O8	1.953(3)	P2–O4	1.562(3)
Mo2–O11	1.983(3)	P3–O19	1.502(3)
Mo2–O5	2.044(3)	P3–O18	1.535(3)
Mo2–O9	2.089(3)	P3–O5	1.562(3)
Mo2–O14	2.286(3)	P3–O6	1.570(3)
Mo3–O3	1.686(3)	Co1–O11	2.142(3)
Mo3–O10	1.945(3)	Co1–O12	2.175(4)
Mo3–O12	1.977(3)	Co2–O18	2.070(3)
Mo3–O6	2.059(3)	Co2–OW1	2.122(3)
Mo3–O9	2.093(3)	Co2–OW2	2.146(3)

purple powder by decantation and washed with water (15% yield in crystals, based on Mo). IR (KBr pellets, ν/cm^{-1}): 1106 (s), 1027 (s), 955 (s), 804 (m), 739 (w), 689 (m), 615 (w), 590 (w), 563 (w), 505 (m). $H_{94}Co_3Mo_{12}Na_{12}O_{106}P_8$: calcd. Co 4.85, Mo 31.62, Na 7.58, P 6.81; found Co 5.20, Mo 30.37, Na 7.08, P 6.56%.

Thermogravimetric analyses were performed on powdered samples on a TA-instrument 2050 thermo-analyser in air over the temperature range 25 to 600 °C (heating rate 5 °C min^{-1}).

X-Ray powder diffraction data were collected in air on a Siemens D5000 diffractometer (Cu Kα radiation).

For single crystals, intensity data collection was carried out with a Siemens SMART three-circle diffractometer equipped with a CCD bidimensional detector using Mo Kα monochromatized radiation ($\lambda=0.71073$ Å). The absorption correction was based on multiple and symmetry-equivalent reflections in the data set using the SADABS program[5] based on the method of Blessing.[6] The structures were solved by direct methods and refined by full-matrix least-squares using the SHELX-TL package.[7] Crystallographic data are given in Table 1. Selected bond distances are listed in Table 2.

CCDC reference numbers 168690 and 168691. See http://www.rsc.org/suppdata/jm/b1/b104030h/ for crystallographic data in CIF or other electronic format.

Magnetic susceptibility measurements were carried out with a Quantum Design SQUID magnetometer with an applied field of 5000 G. The independence of the susceptibility value with regard to the applied field was checked at room temperature.

Results and discussion

Synthesis

The molybdenum phosphates **1** and **2** are synthesized in moderately good yield, starting from a slurry containing Na_2MoO_4, Mo, iminodiacetic acid, H_3PO_4 and MCl_2 (M = Mn, Co). Hydrothermal conditions are required to promote the reduction of Mo^{VI} by Mo, to form the Mo^V dinuclear fragment. Although iminodiacetic acid is not a part of the final product, its presence as reactant is necessary for the crystallization of **1** and **2**. Considering the chelating properties of $[HN(CH_2COO)_2]^{2-}$, a possible role for this ligand may be the formation of an intermediate complex with M^{2+} ions involved in the formation of **1** and **2**. Crystals of **1** and **2** are brown-red, a typical color for compounds containing $\{Mo_2O_4\}$ fragments. The IR spectra of **1** and **2** display similarities although the phosphate bands in the region 1000–1200 cm^{-1} and the Mo=O bands in the region 900–1000 cm^{-1} are split in compound **1** compared to compound **2**. The pH of the reaction has a crucial role in the synthesis. Indeed, compound **1** only forms in a limited pH range (5.5–6), as does compound **2** (5–6). Below pH = 4, light blue crystals of the known mineral hureaulite[8] $Mn_5(HPO_4)_2(PO_4)_2(H_2O)_4$ are quantitatively obtained instead of **1**.

Structure description

The common building unit in **1** and **2** is the $[P_4Mo_6O_{28}(OH)_3]^{9-}$ anion (P_4Mo_6) (Fig. 1a). As is usually observed,[2,3] the Mo^V atoms are dimerized, forming $\{Mo_2O_4\}$ units. In P_4Mo_6, three $\{Mo_2O_4\}$ units are mutually connected by a peripheral phosphato ligand and by a hydroxo group. The six molybdenum atoms are coplanar and display alternating short (approximately 2.6 Å) Mo–Mo bonds within the $\{Mo_2O_4\}$ units, and longer (approximately 3.5 Å) non-bonding contacts between the building blocks, which is a common feature in cyclic arrangements based on dinuclear $\{Mo_2O_2E_2\}$ (E = O, S) units.[2,3] The connections between each building unit are edge-sharing. The resulting hexanuclear ring encapsulates a central

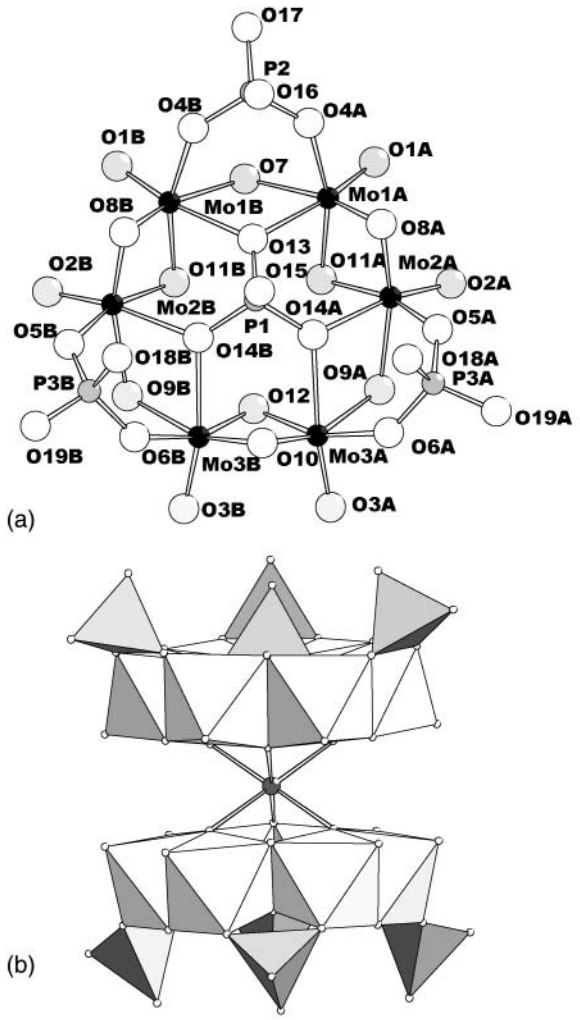

Fig. 1 a) Ball and stick representation of the anionic building unit P_4Mo_6 with atom-labeling scheme; in **1** the asymmetric unit consists of the whole polyanion, with two fragments labeled A, B, while in **2** the anion lies on a mirror plane and the asymmetric unit consists of only one fragment; b) side view of the dimeric unit formed by two P_4Mo_6 bridged by a Mn^{2+} or Co^{2+} ion in **1** or **2** respectively.

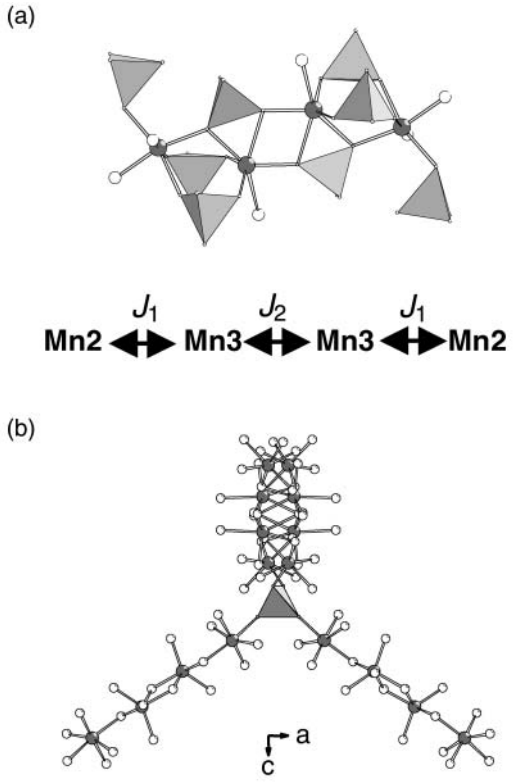

Fig. 2 a) Scheme of coupling within the Mn^{II} tetramer; b) view of the tetramers of Mn^{2+} connected *via* the extra phosphate group in **1**.

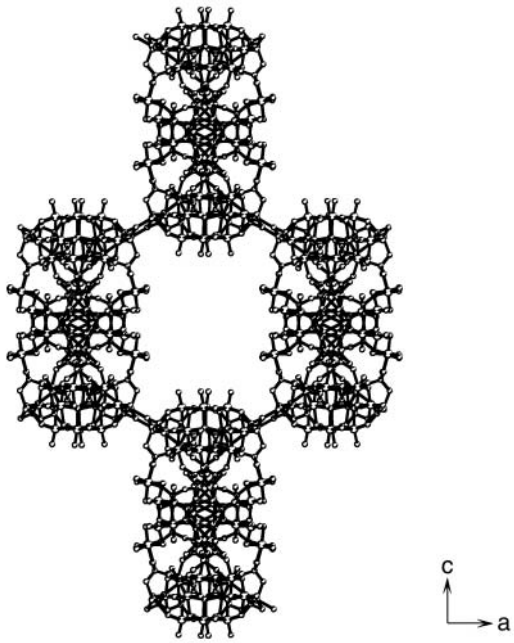

Fig. 3 View along [010] of the polyanions directly connected to the grid formed by the manganeso-phosphate skeleton in **1**.

phosphate group. The central and the three peripheral phosphate groups lie on the same side of the plane defined by the six molybdenum atoms (Fig. 1b). An M^{2+} (M = Mn in **1**, Co in **2**) ion in regular octahedral coordination links two P_4Mo_6 anions *via* three (μ-O) atoms (O11, O12) of the three $\{Mo_2O_4\}$ units (Fig. 1b). The formation of such dimeric species has often been encountered either with encapsulated transition metal cations[2c,e–i] or alkaline cations.[2a] Valence bond calculations have been performed, confirming the protonation of the oxo bridges (O7, O9). In **2**, the sandwich $Co(P_4Mo_6)_2$ unit has thus a −16 charge and the electrical balance is ensured by the presence of twelve sodium cations and two extra cobalt ions, as confirmed by the elemental analysis and the structure determination. In **1**, an additional proton, probably delocalized over the three peripheral phosphato groups, has to be added in order to satisfy the electroneutrality of the compound.

In **1**, four Mn^{2+} atoms are bridged by phosphato groups of the P_4Mo_6 anions forming a tetramer of manganese (Fig. 2a), all the Mn(II) ions being in a highly distorted octahedral environment (Table 2). This has been previously observed for manganese phosphate compounds.[9] The Mn2 and Mn3 ions ($d_{Mn2–Mn3} = 3.76$ Å) are bridged by one μ_3-O atom and two phosphato groups *via* four μ-O atoms, and the two Mn3 ions ($d_{Mn–Mn} = 3.65$ Å) are bridged by two μ_3-O atoms. A terminal water molecule completes the coordination sphere of each manganese. A noteworthy feature in the structure of **1** is the presence of an extra PO_4 group, lying on a $\bar{4}$ axis, besides the four phosphato groups constituting the P_4Mo_6 anion. This phosphato group connects four tetramers of manganese (Fig. 2b), thus playing a key role as a structure directing agent. The manganese phosphate skeleton forms a regular grid to which P_4Mo_6 anions are anchored (Fig. 3).

The three-dimensional structure of **2** appears quite different. Considering that the experimental conditions are strictly similar for **1** and **2**, this implies that the three-dimensional structure is strongly dependent on the nature of the transition metal. In **2**, a Co^{2+} ion connects two $Co(P_4Mo_6)_2$ units *via* the

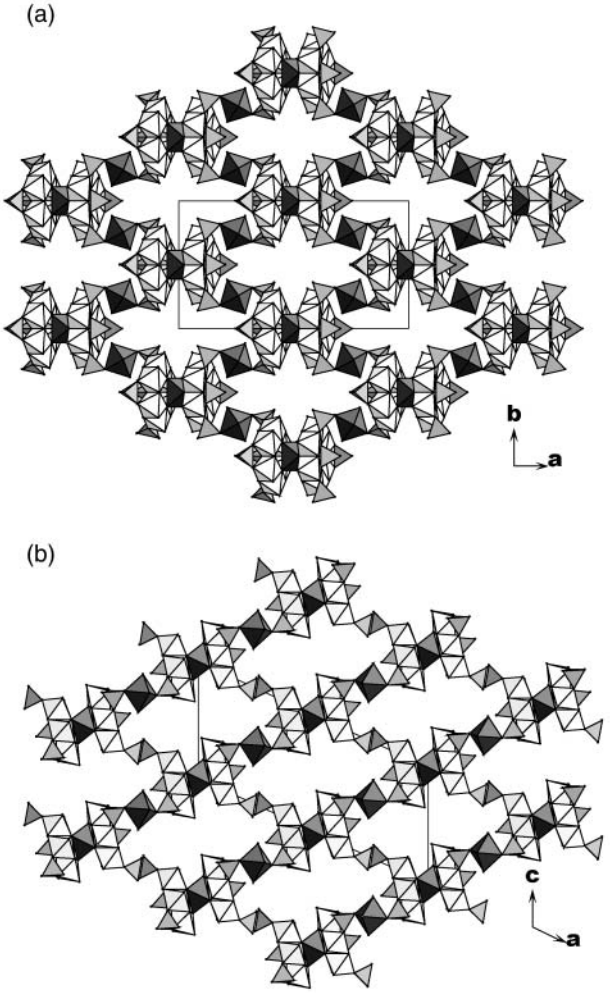

Fig. 4 View of the channels running along [001] (a) and [010] (b) in **2**. Sodium and water molecules have been omitted for clarity.

oxygen O18 of two peripheral phosphato groups. The resulting three-dimensional anionic framework delimits channels running along the [001] and [010] axes (Fig. 4). The connectivity scheme between the $Co(P_4Mo_6)_2$ units in **2** is highly reminiscent of that observed between the $Fe(P_4Mo_6)_2$ units in $(TMA)_2(NH_4)_2[Fe_2Mo_{12}O_{30}(H_2PO_4)(HPO_4)_2]\cdot 11H_2O$.[2d] In the latter structure, the charge-compensating cations are ammonium and tetramethylammonium cations while in **2** disordered sodium atoms act as counter-ions in the structure and form an intricate network. The sodium atoms are linked to water molecules and to oxygen atoms of the P_4Mo_6 anion and are segregated in two sodium clusters (Fig. 5a). These sodium clusters exactly fill the cavities designed by the anionic network (Fig. 5b) leading to a compact structure. Compound **2** is highly hydrated, as confirmed by the thermogravimetric analysis (TGA), which displays a weight loss of 16.2% in the temperature range 25–100 °C and 21.2% in the temperature range 25–300 °C, corresponding to the release of all the water molecules (calculated 21.7%). Consequently, the three-dimensional framework easily collapses as shown by the absence of diffraction peaks in the thermodiffractogram of **2** and the non-reversible color change after a sample of **2** has been heated at 300 °C.

Magnetic properties

The Co^{2+} ions in **2** are isolated from one another and are therefore not expected to be coupled. Thus, only the magnetic properties of **1** have been investigated. The results are shown in Fig. 6 in the forms of $\chi_M T$ *versus* T and $1/\chi_M$ *versus* T plots.

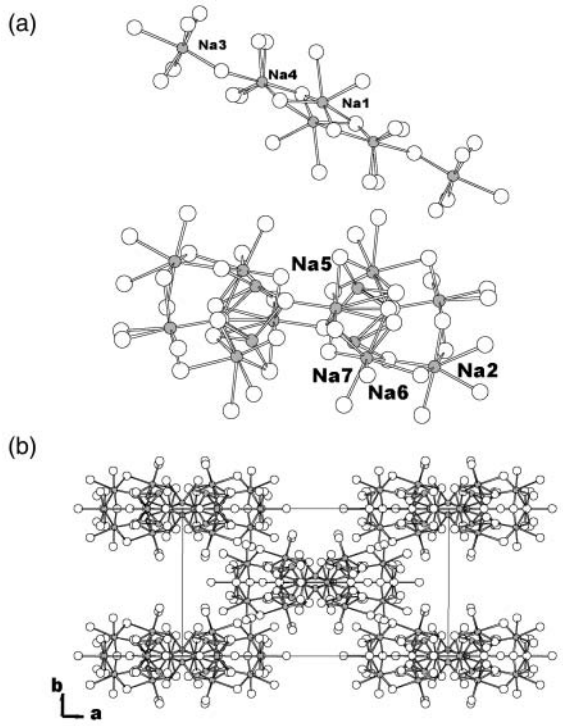

Fig. 5 a) Representation of the two clusters of disordered sodium atoms in **2**; b) view of the sodium clusters in the unit cell, filling the holes delimited by the anionic framework.

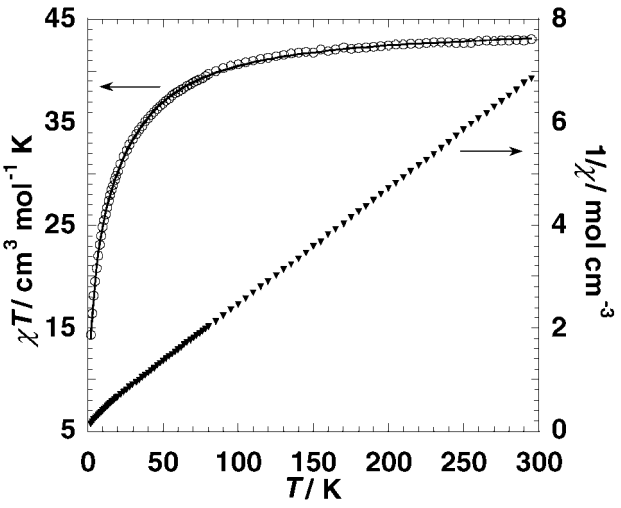

Fig. 6 Thermal dependence of $\chi_M T$ and $1/\chi_M$ for **1**. The solid line was generated from the best fit parameters given in the text.

Between 300 and 30 K, the $1/\chi_M = f(T)$ curve can be fitted by a Curie–Weiss law $1/\chi_M = (T-\theta)/C_m$, where $C_m = 44.55\ cm^3\ mol^{-1}\ K$ and $\theta = -10.05$ K. This value of θ is indicative of antiferromagnetic exchange interactions between the Mn(II) cations in **1**. The $\chi_M T$ curve exhibits a continuous decrease upon cooling from 300 K ($\chi_M T = 43.04\ cm^3\ mol^{-1}\ K$) to 2 K ($\chi_M T = 14.34\ cm^3\ mol^{-1}\ K$). As Mn(II) ions which link two P_4Mo_6 anions can be considered as isolated, only the coupling between the manganese atoms forming the chains has to be taken into account. Moreover, in order to establish the Heisenberg Hamiltonian relative to compound **1**, the more realistic approximation to the problem is to consider only magnetic interactions arising between manganese sharing oxygen atoms, neglecting the interaction between manganese atoms linked *via* the long O–P–O bridge ($d_{Mn-Mn} = 5.672$ Å).

This approximation leads to the study of interactions in a linear tetrameric species of Mn(II). Due to the presence of an inversion center, this tetramer can be described as a pair of dimers. It follows that only two coupling constants J_1 and J_2 have to be considered, as depicted in Fig. 2a. We then used the following Heisenberg Hamiltonian to analyze the magnetic data:

$$\hat{H}_S = -J_1(\hat{S}_1\hat{S}_2 + \hat{S}_3\hat{S}_4) - J_2\hat{S}_2\hat{S}_3 \quad (1)$$

where $S_i = 5/2$ is the value of the spin for Mn^{II}_i. There is no analytical solution for the eigenvalues of this Hamiltonian, the only good quantum number being the total spin. Thus, the eigenvalues of $\hat{H}_S$ have been calculated by diagonalizing the full 6^4 spin problem. The magnetic susceptibility was calculated using Van Vleck's formula. The best fit was found for $g = 2.018$, $J_1 = -1.09\ cm^{-1}$ and $J_2 = -3.65\ cm^{-1}$ ($R = 1.14 \times 10^{-5}$).[10] To our knowledge, no exchange coupling constants have been calculated for other tetrameric Mn(II)-phosphate species. Nevertheless, two Mn(II)-phosphates have been recently reported and their magnetic properties studied and interpreted by fitting the experimental data to trinuclear species. For these two compounds, an antiferromagnetic interaction was found between the Mn(II) ions. For the linear trinuclear manganese phosphate $Mn_3(H_2O)_6Ga_4(PO_4)_6$,[9] where the Mn(II) ions in an octahedral environment are edge-sharing, the J value has been found equal to $-3.35\ cm^{-1}$. For the complex $\{Mn_2(HPO_4)_3(H_2O)\}$,[11] the structure consists of MnO_5 trigonal pyramids and edge-sharing octahedral MnO_6. The data were fitted considering a triangular arrangement of Mn(II), with $J = -0.5\ cm^{-1}$. The values of J found for compound **1** are then consistent with these results, and characteristic of the relative weakness of the magnetic interactions between Mn(II) ions.

In conclusion, two new three dimensional solids composed of Mn^{II} (**1**) or Co^{II} (**2**) and Mo^{V} phosphates based on the same $[P_4Mo_6O_{28}(OH)_3]^{9-}$ anionic building group have been obtained and characterized crystallographically. **1** can be considered as the first compound associating infinite chains of transition metals and P_4Mo_6 building groups. A magnetic study has revealed that the Mn^{2+} ions are antiferromagnetically coupled. Substitution of one metal by another does not result in isostructural compounds, showing that the three-dimensional structure is strongly dependent on the nature of the transition metal.

Acknowledgements

We thank Dr. C. Livage for fruitful discussions.

References

1 See for a review R. C. Haushalter and L. A. Mundi, *Chem. Mater.*, 1992, **4**, 31.
2 (*a*) R. C. Haushalter and F. W. Lai, *Angew. Chem., Int. Ed. Engl.*, 1989, **28**, 743; (*b*) R. C. Haushalter and F. W. Lai, *Inorg. Chem.*, 1989, **28**, 2905; (*c*) L. A. Mundi and R. C. Haushalter, *Inorg. Chem.*, 1992, **31**, 3050; (*d*) L. A. Mundi and R. C. Haushalter, *Inorg. Chem.*, 1993, **32**, 1579; (*e*) P. Lightfoot and D. Masson, *Acta Crystallogr., Sect. C*, 1996, **52**, 1077; (*f*) L. Xu, Y. Sun, E. Wang, E. Shen, Z. Liu and C. Hu, *J. Solid State Chem.*, 1999, **146**, 533; (*g*) L. Xu, Y. Sun, E. Wang, E. Shen, Z. Liu, C. Hu, Y. Xing, Y. Lin and H. Jia, *New J. Chem.*, 1999, **23**, 1041; (*h*) A. Guesdon, M. M. Borel, A. Leclaire and B. Raveau, *Chem. Eur. J.*, 1997, **3**, 1797; (*i*) A. Leclaire, A. Guesdon, F. Berrah, M. M. Borel and B. Raveau, *J. Solid State Chem.*, 1999, **145**, 291.
3 E. Cadot, A. Dolbecq, B. Salignac and F. Sécheresse, *Chem. Eur. J.*, 1999, **5**, 2396.
4 C. du Peloux, A. Dolbecq, P. Mialane, J. Marrot, E. Rivière and F. Sécheresse, *Angew. Chem., Int. Ed.*, 2001, **40**, 2455.
5 G. M. Sheldrick, SADABS, program for scaling and correction of area detector data, University of Göttingen, Germany, 1997.
6 R. Blessing, *Acta Crystallogr., Sect. A*, 1995, **51**, 33.
7 G. M. Sheldrick, SHELX-TL version 5.03, Software Package for the Crystal Structure Determination, Siemens Analytical X-ray Instrument Division, Madison, WI, USA, 1994.
8 (*a*) P. B. Moore and T. Araki, *Am. Mineral.*, 1973, **58**, 302; (*b*) S. Menchetti and C. Sabelli, *Acta Crystallogr., Sect. B*, 1973, **29**, 2541; (*c*) Y. Gerault, A. Riou and Y. Cudennec, *Acta Crystallogr., Sect. C*, 1987, **43**, 1829; (*d*) H. S. D. Amorim, H. R. D. Amaral Jr., L. F. Moreira and E. Mattievich, *J. Mater. Sci.*, 1996, **15**, 1895.
9 K.-F. Hsu and S.-L. Wang, *Inorg. Chem.*, 2000, **39**, 1773.
10 $R = [\Sigma(\chi_M T_{calc} - \chi_M T_{obs})^2 / \Sigma(\chi_M T_{obs})^2]$.
11 J. Escobal, J. L. Pizarro, J. L. Mesa, L. Lezama, R. Olazcuaga, M. I. Arriortua and T. Rojo, *Chem. Mater.*, 2000, **12**, 376.